Structure–property relationships of polycarbonate diol-based polyurethanes as a function of soft segment content and molar mass

Victor Costa,[1] Andrés Nohales,[1] Paula Félix,[2] Carmen Guillem,[2] David Gutiérrez,[2] Clara María Gómez[2]

[1]R&D Department, UBE Corporation Europe, S.A. 12100 Castellon, Spain
[2]Instituto de Ciencia de los Materiales, Universidad de Valencia, 46980 Paterna Valencia, Spain
Correspondence to: C. M. Gómez (E-mail: clara.gomez@uv.es)

ABSTRACT: Segmented thermoplastic polyurethanes (PUs) have been synthesized with polycarbonate diol as soft segment and 4,4′-diphenylmethane diisocyanate and butanediol as hard segment. Two different series employing two different soft-segment molar mass, 1000 and 2000 g/mol, and by changing the hard-segment content from 32 to 67% have been investigated with the aim to elucidate the effect of the different content variations on the properties. Morphological, thermal, and mechanical properties have been studied by Fourier transform infrared spectroscopy (FTIR), differential scanning calorimetry (DSC), dynamic mechanical analysis (DMA), wide angle X-ray diffraction, atomic force microscopy, tensile and tear strength, hardness, and specific gravity tests. Properties have been explained from the standpoint of miscibility between hard- and soft-segment microdomains of the tailored segmented PUs through an exhaustive analysis. FTIR, DSC, and DMA measurements revealed that miscibility between hard and soft microdomains increases as the molar mass of the macrodiol decreases. An increase in hard-segment content entailed the formation of larger hard domains with higher crystallinity what results in superior mechanical properties such as higher tensile stress and tear strength, and hardness. © 2014 Wiley Periodicals, Inc. J. Appl. Polym. Sci. **2015**, *132*, 41704.

INTRODUCTION

Nowadays, polyurethanes (PUs) are among the most important class of specialty polymers. They contain urethane groups in the molecular backbone regardless of the chemical composition of rest of the chain and are used in many different commercial applications such as rigid or flexible foams, elastomers, coatings, adhesives, or sealants.[1–3]
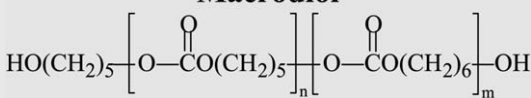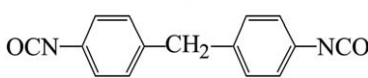
More precisely, segmented thermoplastic PUs constitute a kind of linear block copolymers formed by alternating hard and soft segments.[3–12] The soft segment block is, generally, a dihydroxy-terminated macromolecular chain of medium molar mass (from 500 to 3000 g/mol) with a glass transition temperature, T_g, below room temperature that imparts elastomeric properties. The hard segment is formed by the reaction of a diisocyanate with a low molecular mass diol leading to the urethane functionality.[2–6] Segmented PUs display phase-segregated morphologies due to the thermodynamic incompatibility between hard and soft segments.[4–10] The hard segment displays strong hydrogen bonding between the urethane type hard segments, and thus, a physically cross-linked network is formed. Polyurethane properties are a combination of the hardness due to strong hydrogen bonded hard segments with elastomeric properties owing to the continuous soft phase in between the hard domains. Consequently, based on their interactions, the final structure and properties are related to the partial solubility between hard and soft segments.[1–12]

Overall, chemical and physical properties of segmented PUs depend on a combination of multiple factors, such as molecular structure and molar mass of every component (diisocyanate, polyol), hard-to-soft segment ratio, and manufacturing conditions.[7–12] Focusing on the soft segment, macrodiols, such as polyether and polyester polyols, are the most employed and studied in the literature.[7,9,11,13–15] However, for applications, which require high water, heat resistance, and high mechanical strength, polycarbonate diol (PCD)-based PUs are preferred.[5,7,10,15,16] The effect of the structure and characteristics of polycarbonate diols on PU properties have been scarcely investigated and many questions related to structure–property correlations still remain unsolved.

The aim of this work is to synthesize thermoplastic PUs based on polycarbonatodiol as soft segment and to investigate the

Table I. Main Characteristics of the Reagents Used

Chemicals	Molar mass (g/mol)	T_g [a] (°C)	T_f (°C)	State at 25°C
Macrodiol Polyhexamethylene-pentamethylen carbonate diol, Eternacoll® PH	1000 2000	−58.1 −52.1	– –	Viscous liquid
Diisocyanate 4,4′-diphenylmethane diisocyanate, MDI	250.26	–	49	White solid
Chain extender 1,4-Butanediol, BD	90.12	–	20	Liquid

[a] From differential scanning calorimetry first scan.

influence of the macrodiol molar mass and of the hard-segment content on its properties. The effect of specific interactions and PCD molar mass on the structure and properties of the PUs are investigated. Two copolymers of polyhexamethylene–pentame-thylen carbonate diol of molar masses 1000 and 2000 g/mol are used in this work as the soft phase. Different PU stoichiometries hard to soft segments phases from 32 to 67% weight percentage have been synthesized to understand variations of microdomain composition on properties. Physicochemical, morphological and mechanical behaviors were analyzed as a function of the poly-carbonatediol molar mass and hard-segment content.

EXPERIMENTAL

Material

In this study, we have prepared two series of segmented PUs with three hard-segment contents by changing the molar mass of the soft segment. The hard segment consists of 4,4′-diphenyl-methane diisocyanate, MDI, and 1,4-butanediol, BD, as chain extender which were obtained from Sigma Aldrich. The soft segment is polyhexamethylene-pentamethylen carbonate diol, Eternacoll®PH, with two different molar masses, 1000 and 2000 g/mol, kindly supplied by UBE Chemical Europe. The main characteristics such as formulae, composition, molecular weight, melting and glass transition temperatures, T_m and T_g, respectively, and physical state at room temperature are pre-sented in Table I. Dimethyl acetamide (DMAc) from Aldrich was used as solvent. All materials were kept in a dry box to avoid humidity.

Polyurethane Synthesis

Polyurethane solution was prepared via a two-step, prepolymer synthesis method.[5] In the first step, polycarbonate diol and excess of diisocyanate, previously dissolved in DMAc, were poured in a reactor at a temperature of 70°C during 1 h in an argon atmosphere to form a prepolymer of polycarbonate diol endcapped with diisocyanate groups. In the second step, buta-nediol dissolved in DMAc was added to the prepolymer at 60°C, and the mixture was kept at 70°C for 1 h to obtain the polyurethane solution. The PU solution was cast on a glass plate, at room temperature, with the aid of a film application mechanical machine Neurtek RK Control coater. The solvent was evaporated in an oven at 80°C during 24 h. The thickness of the obtained films was of 0.1–0.2 mm. The nomenclature used, reagents molar ratio, and hard-segment content (f) of the samples are summarized in Table II.

Characterization

Fourier transform infrared-attenuated total reflection spectros-copy (FTIR-ATR) measurements were performed with a Thermo Nicolet Nexus-FTIR spectrometer provided with a multiple internal reflection accessory ATR single bounce. Samples were pressed against ATR accessory diamond crystal by means of the fixing screw using a flat tip. Single-beam spectra of the samples were obtained at room temperature after averaging of 124 scans between 4000 and 400 cm^{-1} with a resolution of 4 cm^{-1}. All spectra were obtained in the transmittance mode. Infrared car-bonyl region of polyurethane samples were resolved into four Gaussian curves using Origin-Pro-7.5 software with an average half height peak width of 20 cm^{-1}.

Differential scanning calorimetry (DSC) scans were performed using a TA Instrument Q20 equipped with a refrigerated cool-ing system and nitrogen purge. Calibration was performed with indium according to manufacturer recommended procedures. About 5–7 mg of sample was sealed in an aluminum pan for every test. Thermal behavior was investigated by scanning the samples from −90 to 230°C at a heating rate of 20°C/min. The midpoint of the heat capacity change has been chosen to

Table II. Compositional Characteristics of Polyurethane Microdomains in the Initial Synthesis and as Obtained by FTIR Analysis.

System	PH/MDI/BD molar ratio	f	X_b	$w_{H,FTIR}$	$w_{H,FTIR}/f$
PUPH100-37	1 : 2 : 1	0.37	0.17	0.33	0.88
PUPH100-48	1 : 3 : 2	0.48	0.33	0.38	0.80
PUPH100-62	1 : 5 : 4	0.62	0.37	0.51	0.81
PUPH200-32	1 : 3 : 2	0.32	0.25	0.26	0.81
PUPH200-49	1 : 6 : 5	0.49	0.45	0.34	0.70
PUPH200-60	1 : 9 : 8	0.60	0.46	0.45	0.75

f is the hard-segment weight fraction in the polyurethane from initial reactants compositions. X_b is the fraction of hydrogen-bonded urethane carbonyl groups and $w_{H,FTIR}$ is the hard-segment weight fraction of the overall soft phase from FTIR data.

represent the glass transition temperature, T_g, and melting point refers to the endotherm peak temperature.

Dynamic mechanical analysis (DMA) was performed on a DMA 2890 model of TA instruments. Calibration was performed as per manufacturer recommendations included in TA software. The experiments were conducted in tensile mode, and the specimen dimensions were of 16 mm length, 6 mm thick, and 0.2 mm width. A constant heating rate of 3°C min^{-1} over a temperature range of -100–180°C was applied in all the tests. These experiments yield the storage modulus (E'), the loss modulus (E'') and the damping factor tan δ ($=E''/E'$). The T_g was determined from the peak temperature of the tan δ curve.

Wide angle X-ray diffraction was measured using a Seifert XRD 3003 TT diffractometer. The X-ray beam was Ni-filtered CuKα radiation from a sealed tube operated at 40 KV and 40 mA. The data collection was recorded in the 2θ range of 4°–40° with a scanning interval of 0.08°.

Tapping Mode Atomic Force Microscopy. Phase and topography images were captured at room temperature using a Nanotech equipment at integrated force generated by cantilever/silicon probes, by applying a resonance frequency of 330 kHz. Cantilever silicon/probes had a tip radius less than 10 nm and 125 μm long. This technique was used for the morphological analysis of the free surface growth.

Tensile properties were measured at 23°C on five replicates of each material using an Instron Model 5566 Universal Testing machine according to standard "ISO 527-1 : 1993. Plastics. Determination of tensile properties." A 5 kN load cell was used, and the crosshead speed was 300 mm/min. Pneumatic grips were required to hold the test specimens.

Measurements of the tear strength were performed with an Instron Model 5566 Universal Testing machine according to standard "ISO 34-1 : 2004. Rubber, vulcanized or thermoplastic. Determination of tear strength." A 5 kN load cell was used, and the crosshead speed was 500 mm/min. Pneumatic grips were required to hold the test specimens.

Polyurethanes hardness measurements were taken by using a Zwick Roell durometer following "UNE-EN ISO 868 : 1998: Plastics and ebonite. Determination of indentation hardness by

means of a durometer (Shore hardness)" standard procedure at 23°C. In this work, we have used two types of indenter, "Shore A and Shore D," depending on the samples hardness.

Measurements of specific gravity were obtained according to the JIS K 7311 "Testing methods for thermoplastic PU elastomers" using a chemical balance KERNT-ALT100-4M, provided with a solid density determination set.

RESULTS AND DISCUSSION

Thermoplastic segmented PUs based on hexamethylene-pentamethylene carbonate diol (PH) of molar mass 1000 and 2000 g/mol and three different hard-segment contents are synthesized and characterized by different techniques to understand structure-properties relationships.

Infrared analysis has been used to study hard–hard and hard–soft segment interactions by H-bonding at room temperature.[5,8,11–13,17–20] Figure 1 shows the FTIR spectra in different wavelength regions of the PUs studied. Two characteristic vibrational regions, the N—H stretching vibration (3200–3500 cm^{-1}) and the carbonyl absorption region (1630–1730 cm^{-1}), are analyzed to investigate the degree of hydrogen bonding in PUs. The shift of these peaks to lower frequency results from the weakening of the bonds between N—H and C=O due to hydrogen bonding. The inspection of the —N—H stretching region for the systems under study [Figure 1(a,b)] reveals no noticeable peak about 3446 cm^{-1} characteristic of non-H-bonded-N—H groups.[17] However, a peak around 3300 cm^{-1} that is attributed to the H-bonded —N—H groups is clearly distinguished. The peak wavelength moves to lower values as the hard-segment content increases. Simultaneously, the area of this peak, A_{NH}, with respect to the —CH-stretching vibration (2940–2865 cm^{-1}) increases as the hard-segment content increases. That is $A_{NH}/A_{CH2} = 0.43$, 0.64, and 0.86 for PUPH100-37, PUPH100-48, and PUPH100-62 and $A_{NH}/A_{CH2} = 0.47$, 0.70, and 0.86 for PUPH200-32, PUPH200-49, and PUPH200-60, respectively. These results suggest a higher degree of NH interaction by H-bonding as the content of hard segment increases.[18]

In addition, the urethane C=O stretching vibration in the amide-I region is commonly used to determine the extent of microdomains formation due to C=O...H—N bonding [Figure
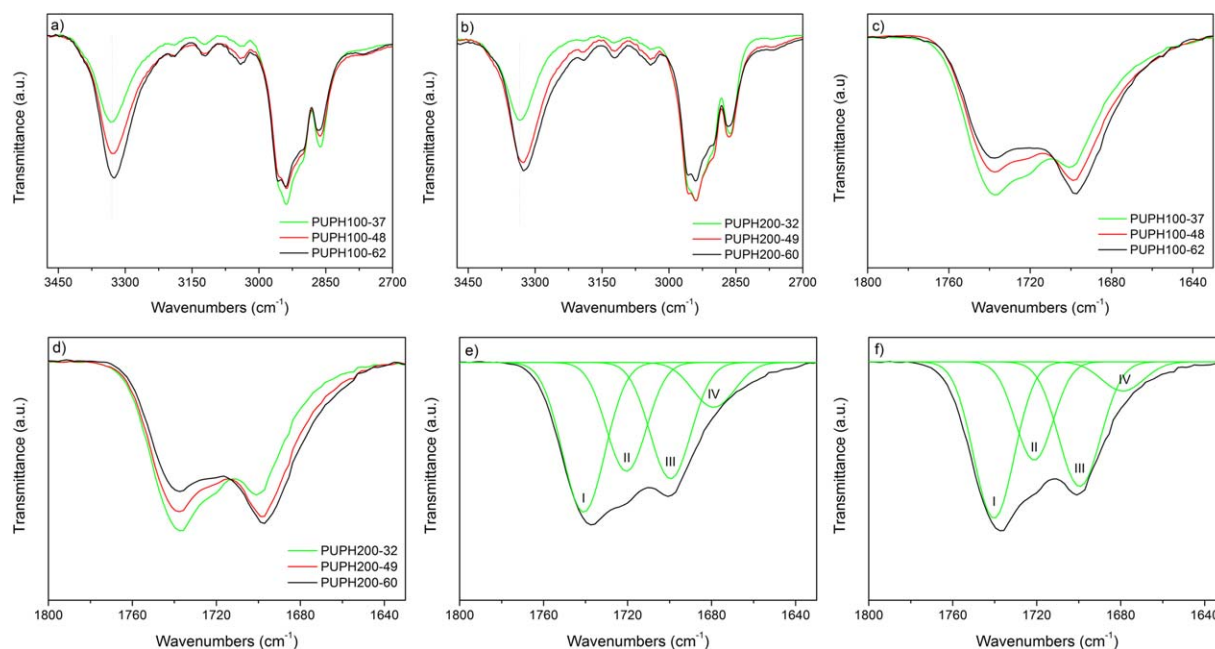
Figure 1. Fourier transform infrared-attenuated total reflection spectra showing the carbonyl absorbance region. [Color figure can be viewed in the online issue, which is available at wileyonlinelibrary.com.]

1(c,d)]. For polycarbonate diol–based PUs, the carbonyl absorption region (1630–1760 cm^{-1})[17,19] can be split in four contributions: (1) band I at 1741 cm^{-1} corresponding to free carbonates; (2) band II at 1720 cm^{-1} for associated carbonates; (3) band III at 1700 cm^{-1} for free urethanes; and (4) band IV at 1685 cm^{-1} for associated urethanes.[7,10,18,20] The iteration procedure of damping least squares curve fitting has been used to separate the absorption peaks in the carbonyl region corresponding to the four kinds of hydrogen-bonding absorption peaks as shown in Figure 1(e,f) as an example for PUPH100-37 and PUPH200-32 as green curves.

The same trend is observed for all the systems independently of molar mass. The absorbance of band I and band II decrease, while the absorbance of band III and band IV increases as the hard-segment content increases. Therefore, the extent of interurethane interaction increases with the hard-segment content. Additionally, band III and IV shift to lower wavelengths with the hard-segment content, indicating an increase in H-bonding urethane association [Figure 1(c,d)].

For further investigation, the ratio between absorbance of the two urethane carbonyl peaks give an idea of the fraction of hydrogen bonded urethane carbonyl groups, X_b. The corresponding absorbance ratio by assuming that the material is isotropic is given by the following equation[7]

$$\frac{A_b}{A_f} = k \frac{X_b}{1-X_b} \tag{1}$$

where A_b is the area of the bonded carbonyl urethane groups, band IV, and A_f is the area corresponding to the free carbonyl urethane groups, band III. The factor ($k = (\varepsilon_b/\varepsilon_f) = 1.2\ \varepsilon_b/\varepsilon_f$) is the relation between the absorption coefficient of bonded carbonyl urethane groups and the absorption coefficient of free carbonyl urethane groups.[7,17]

The weight fraction of hard segment in the soft phase, $w_{H,FTIR}$, determined by FTIR analysis by assuming that H-bonded carbonyl exits only in hard-segment domains, can be calculated from[7]

$$w_{H,FTIR} = \frac{(1-X_b)f}{[(1-X_b)f + (1-f)]} \tag{2}$$

being f the hard-segment weight fraction in the polymer from initial molar ratios (Table II).

Table II summarizes compositional characteristics of PUs as obtained from FTIR analysis. It is observed an increase in the fraction of hydrogen-bonded urethane carbonyl groups, X_b, and of the hard-segment weight fraction of the overall soft phase, $w_{H,FTIR}$, as the hard-segment content increases for both systems differing on macrodiol molar mass, suggesting an increase in hard-domain ordering. These values are lower than the hard-segment values, f, calculated from initial molar compositions. These results are a consequence of hard-segment association due to hydrogen bonding and partial miscibility of hard segment in the soft segment phase. M Spirkova et al.[20] reported an increase in the hard-segment association as the hard-segment content of the polyurethane increases. Values of X_b obtained for the system PUPH200 are very similar to the ones reported by Fernandez d'Arlas et al.[7] for PUs based on poly(hexamethylene carbonate-co-caprolactone) as macrodiol of molar mass 2000 g/mol. Polyurethanes based on PH200 show higher values of X_b and lower values of $w_{H,FTIR}$ than the ones based on PH100. This tendency indicates an increase in miscibility as the molar mass of the macrodiol decreases. These results are in agreement with data reported by Wang and Cooper.[17] They found for PUs based on poly(tetramethylene oxide) an increase in phase segregation as the molar mass
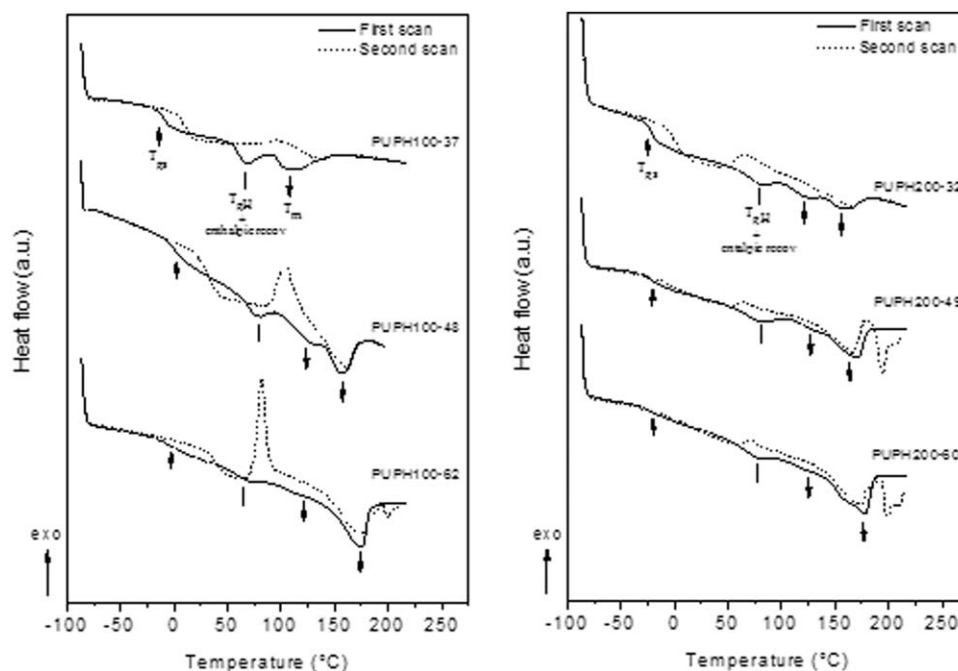
Figure 2. DSC curves for the two systems with different hard-segment content where the arrow up (↑) is glass transition of the soft segment, T_{gs}, line (l) is the overlapping between the glass transition of the hard segment, T_{gH}, and the enthalpic recovery, and the arrows down (↓) are the melting endotherms of crystalline hard microdomains, T_m.

increases from 1000 to 2000 g/mol, similar to the present results.

Thermoplastic PUs exhibit different types of transitions on DSC related with the hard- and soft-segments microdomains. Figure 2 shows DSC thermograms for the different systems assayed. First scan polyurethane thermograms depict a first transition at low temperature associated with the glass transition of the soft segment in the polyurethane, T_{gs}, indicated with arrows up. The second transition is observed around 50–60°C that depending on the sample is observed as a slight change on the slope of the baseline or as a melting endotherm. This transition has been associated with the overlap of the glass transition of hard segment, T_{gH}, with an enthalpy recovery activated by the glass transition.[5,10,13] At higher temperatures, around 120°C and 150°C, several endotherms associated with the melting of hard microdomains are detected and were indicated with arrows down. The first endotherm is related with the interruption of the short-order preceding the melting of crystalline microdomains of hard segment associated with the second endotherm. In both systems, the value of the second endotherm shifts to higher temperatures and the value of the enthalpy associated increases with the hard-segment content which may be related to the formation of longer microdomains of hard segment or structures with greater degree of organization. This trend agrees with the results obtained by Chang et al.[8] and Koberstein et al.[13,14]

In the second scan, there is a glass transition at low temperature, higher than the one observed in the first scan, attributed to the soft segment interacting to a certain extent with the hard

segment, followed by a cold crystallization of the hard segments, and their subsequent melting. Values of T_{gs} in both scans are higher than the ones corresponding to the macrodiol or pure soft segment (Table I) indicating a certain degree of hard- and soft-segment mixing. These values increase after the second scan denoting that the heating process increases miscibility between microdomains. After the glass transition, crystallization exotherms are observed for all the samples. The hard segments have been enclosed into soft microdomains, and during the second heating scan, they crystallize, and subsequently, at slightly higher temperatures, they melt with the corresponding endothermic peak. The area of the crystallization peak increases with the hard-segment content as does the T_g. It could be related with increasing miscibility hard/soft segments, more hard segment is in the soft phase that is able to crystallize after the T_g of the soft phase, as observed by Kultys et al.[12]

Polyurethanes with macrodiol PH100 depict higher values of T_{gs} than the PUs obtained with PH200, fact that implies higher miscibility or soft hard phase mixing. Furthermore, there is a gradual broadening of the glass transition with increasing hard segment which is associated with increased heterogeneity in the soft segment microdomains as observed by other authors.[17]

The difference between glass transition temperature of the soft segment in the polyurethane, T_{gs}, and the glass transition temperature of the pure soft segment, T_{gs^o}, is commonly used to determine phase segregation in PUs (Table III). Values of glass transition temperatures of soft segment in the polyurethane, T_{gs}, can be related to miscibility between both phases, that is, to the hard-segment fraction present in the soft phase, $w_{H,mix}$. Thus, according to the general addition principle that the

Table III. Differences Between Glass Transition Temperature of the Soft Segment in the Polyurethane, T_{gs}, and of the Macrodiol, T_{gs^o}, and Weight Fraction of the Hard Segment According to eq. (3), $w_{H,mix}$, and to eq. (4), $w_{H,Fox}$

System	First scan			Second scan		
	$T_{gs}-T_{gs^o}$ (°C)	$w_{H,mix}$	$w_{H,Fox}$	$T_{gs}-T_{gs^o}$ (°C)	$w_{H,mix}$	$w_{H,Fox}$
PUPH100-37	49	0.33	0.45	68	0.45	0.58
PUPH100-48	58	0.38	0.51	91	0.60	0.72
PUPH100-62	54	0.35	0.48	97	0.64	0.75
PUPH200-32	30	0.21	0.30	54	0.37	0.50
PUPH200-49	29	0.20	0.29	53	0.37	0.49
PUPH200-60	29	0.20	0.29	–	–	–

change in the thermal properties of a one phase system of two linear components is the addition of change in the property of two components through the following equation:[21]

$$T_{gs}=(1-w_{H,mix})T_{gs^o}+(w_{H,mix})T_{gH^0} \qquad (3)$$

where $T_{gH^0}=110°C$ is the glass transition of the hard-segment forms by MDI + BD.

Similarly, the fraction of hard segment present in the soft phase, $w_{H,Fox}$, can be calculated through the Fox equation:[21]

$$\frac{1}{T_{gs}}=\frac{(1-w_{H,Fox})}{T_{gs^o}}+\frac{w_{H,Fox}}{T_{gH^0}} \qquad (4)$$

Table III compiles the difference between glass transition temperature of the soft segment in the polyurethane, T_{gs}, and glass transition temperature of the pure soft segment, T_{gs^o}, and the values of weight fraction of hard segment present in the soft phase, $w_{H,mix}$ and $w_{H,Fox}$, calculated from eqs. (3) and (4) for the first and second scan. For PUPH100-X system, $(T_{gs}-T_{gs^o})$ notably increases for the second scan denoting an increase in miscibility, higher than the corresponding to the PUPH200-X system. Calculated values for w_H with both models to indicate the same trend, an increase in miscibility as the molar mass of soft segment decreases and after the second scan, and for the system PUPH100, values of w_H are higher than the theoretical value leading to an overestimation of the hard-segment content in the soft phase[22,23].

Dynamic mechanical analysis curves have been obtained as complementary experiments. These curves provide information about the viscoelastic properties, and these properties are greatly influenced by the morphology of microdomains. Figures 3 and 4 show the storage modulus, E', the loss modulus, E'', and damping factor tan δ, as a function of temperature for the two systems. DMA profiles are very sensitive to the macrodiol molar mass and hard-segment content. The value of the storage modulus, E', increases with increasing hard-segment content, whereas the maximum peak intensity of the loss modulus, E'', and of the dissipation factor, tan δ, decrease, as also observed by other authors[9,10,24]. The storage modulus variation with temperature shows a significant decrease, sharper for PUPH100-X than for PUPH200-X, associated with the glass transition temperature of the soft segment, α_s, in the dissipation factor.[22,23] All the samples, excepting PUPH100-37, depict an elastomeric plateau that widens with

increasing hard-segment content and macrodiol molar mass. This region extends more in temperature for the PUPH200-X systems. The increase in hard-segment content implies an increase in the chain length of hard segment in the polyurethane, and therefore, an increase in size of the hard-segment microdomains as observed by DSC and FTIR. The microdomains of hard segment in the polyurethane act as physical cross-linking points and provide rigidity to the material, thereby increasing the storage modulus value. For PUPH100-62 and PUPH200-X, a second relaxation, α_r, at
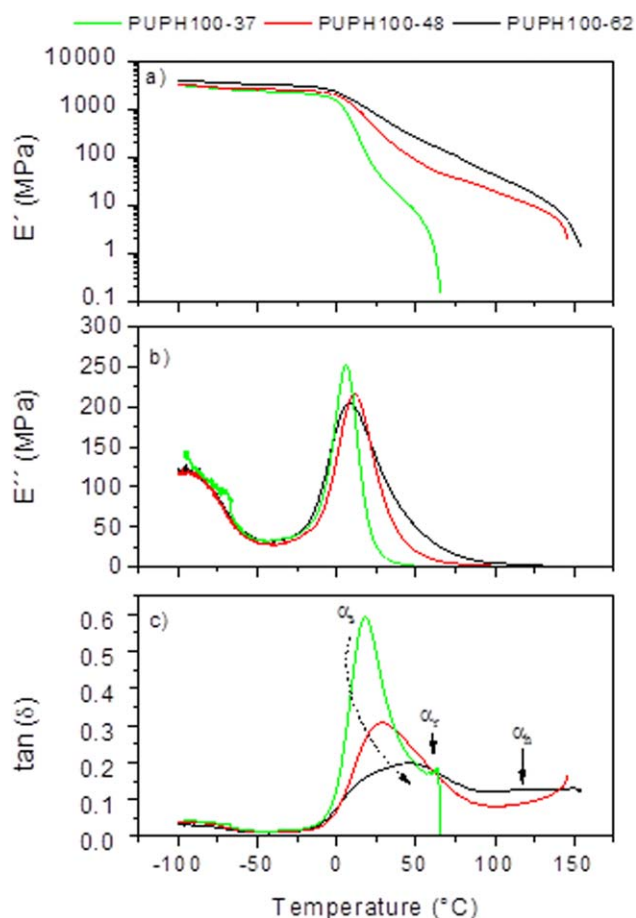

Figure 3. Dynamic mechanical analysis of PUPH100-X PUs: (a) storage modulus, E'; (b) loss modulus, E'', and (c) damping factor, tan δ, as a function of temperature. [Color figure can be viewed in the online issue, which is available at wileyonlinelibrary.com.]
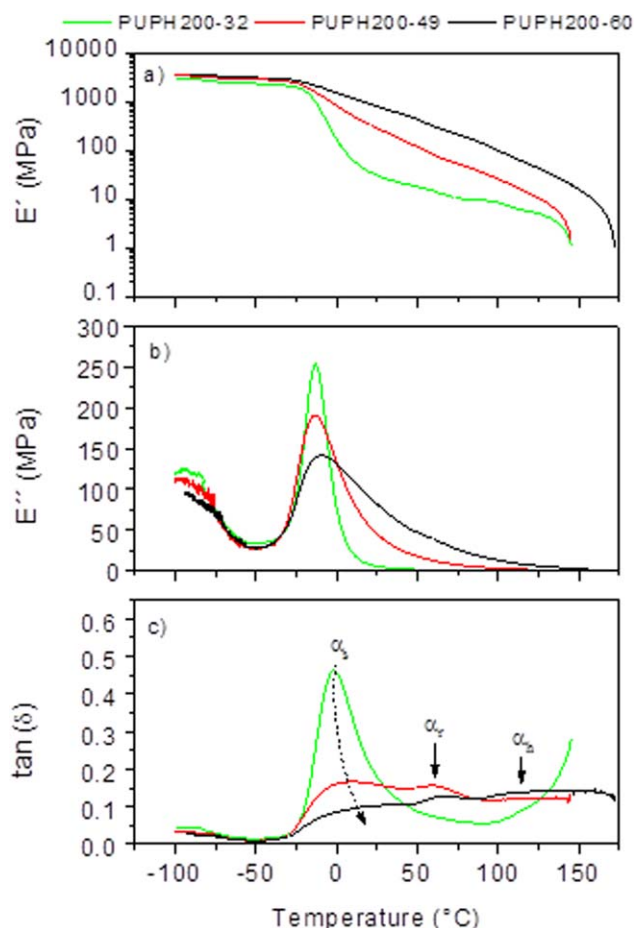
Figure 4. Dynamic mechanical analysis of PUPH200-X PUs: (a) storage modulus, E'; (b) loss modulus, E''; and (c) damping factor, tan δ, as a function of temperature. [Color figure can be viewed in the online issue, which is available at wileyonlinelibrary.com.]

55–70°C in the dissipation factor is observed and has been associated to a second-order type transition of the amorphous contribution of the hard segment.[9,25] Around 110–120°C, for PUPH100-48 and PUPH100-62 and for the system PUPH200-X, a third relaxation in the dissipation factor curve, α_{lp}, occurring with a decrease in the storage modulus is observed. It appears in the same temperature range of the first melting endotherms determined by DSC. This transition is associated with the interruption of short-range order so it could be related to the onset of softening and subsequent melting of the material.[9,25] This temperature increases with increasing hard-segment content as observed in DSC melting endotherm and reported in the literature.[23] By comparing the two systems, it is observed greater phase segregation in the system of higher molecular weight, PUPH200-X, similar to other authors.[17,26]

The X-ray diffraction patterns of the segmented PUs are shown in Figure 5. One large broad diffraction peak at $2\theta = 20°$ can be detected that is associated with the amorphous phase of PUs.[11,27,28] Furthermore, at $2\theta = 11°$ a small peak related with the quasiperiodic arrangement of hard segment is observed.[27,28] This peak located at 11° becomes increasingly evident with increasing hard-segment content. The diffractograms of the samples of both series are characteristic of samples with amorphous nature, although by DSC a certain degree of crystalline structure increasing with the hard-segment content is detected. These results agree with the fact that the signal-to-noise ratio of the X-ray technique is limited, and therefore, the crystalline domains cannot be detected by the instrument, as some authors have reported.[6,29]

Figures 6 and 7 show the morphology of the polyurethane surfaces determined by AFM for the as cast samples. In the phase images (parts a, c and e) clear and bright areas corresponding to the hard segment domains and dark areas corresponding to the soft segment are observed. This morphology,
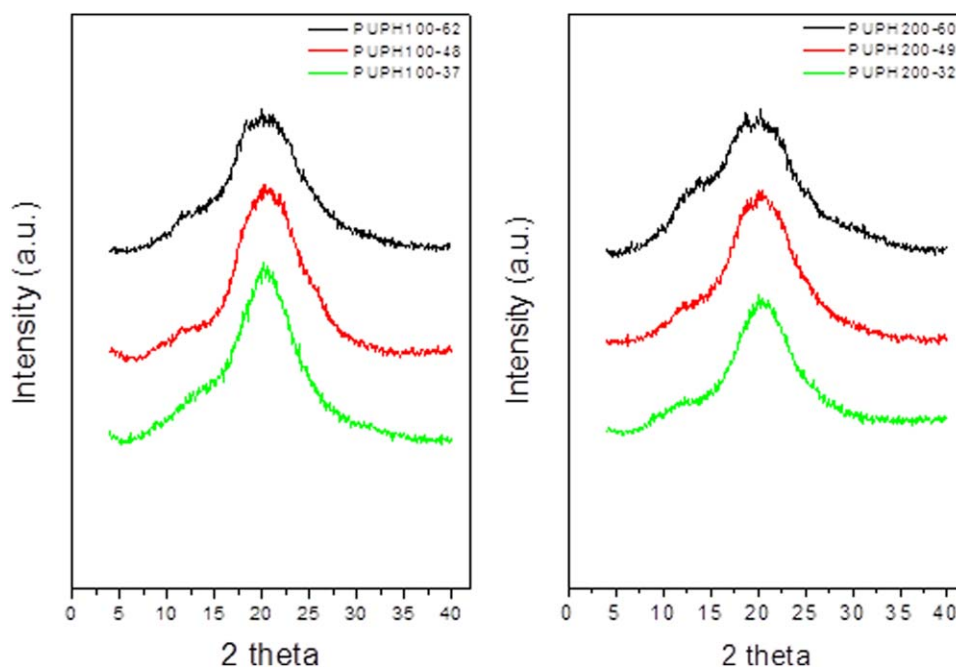

Figure 5. Wide angle X-ray diffractograms of the different PUs. [Color figure can be viewed in the online issue, which is available at wileyonlinelibrary.com.]
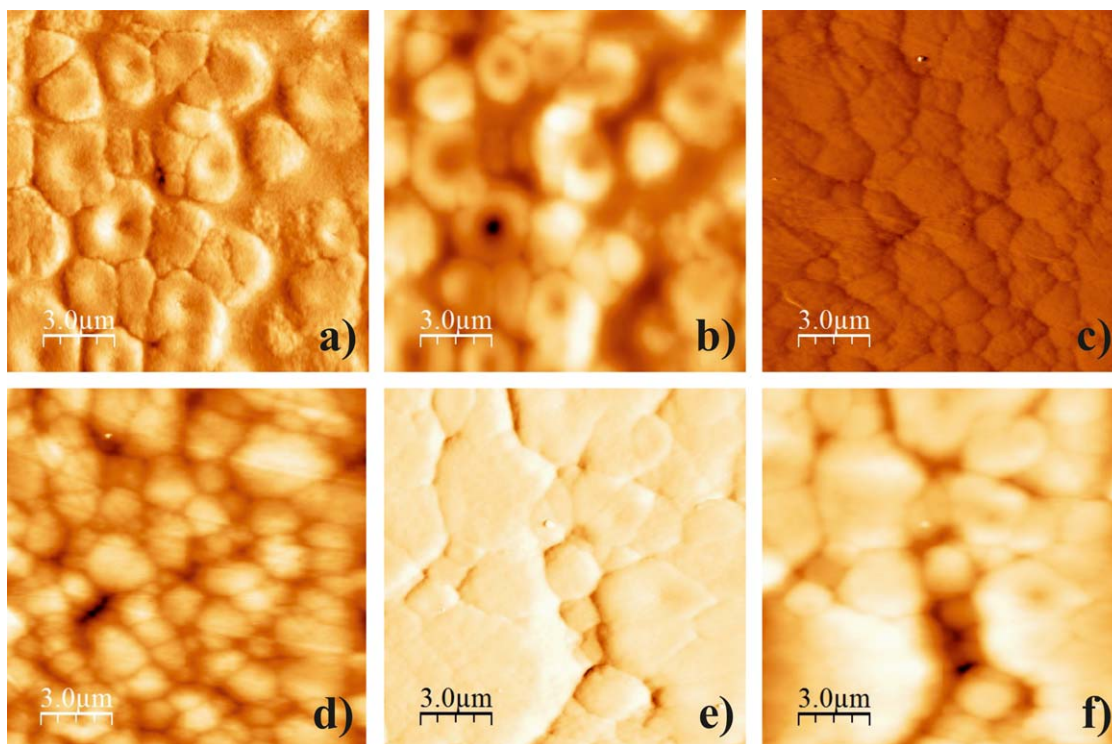
Figure 6. AFM tapping mode images of free surfaces of PUPH100-X as a function of hard-segment content. AFM phase images (a, c, e) and AFM topography images (b, d, f) of free surface samples: (a, b) PUPH100-37, (c, d) PUPH100-48 and (e, f) PUPH100-62. [Color figure can be viewed in the online issue, which is available at wileyonlinelibrary.com.]
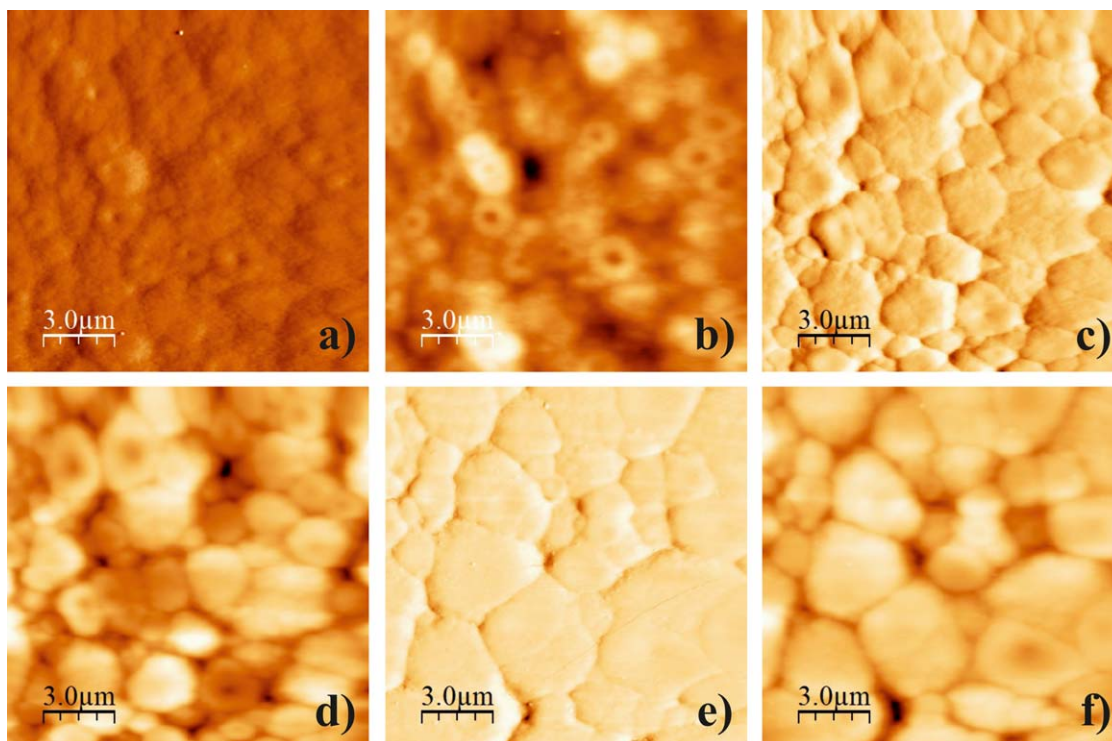

Figure 7. AFM tapping mode images of free surfaces of PUPH100-X as a function of hard-segment content. AFM phase images (a, c, e) and AFM topography images (b, d, f) of free surface samples: (a, b) PUPH200-32, (c, d) PUPH200-49 and (e, f) PUPH200-60. [Color figure can be viewed in the online issue, which is available at wileyonlinelibrary.com.]
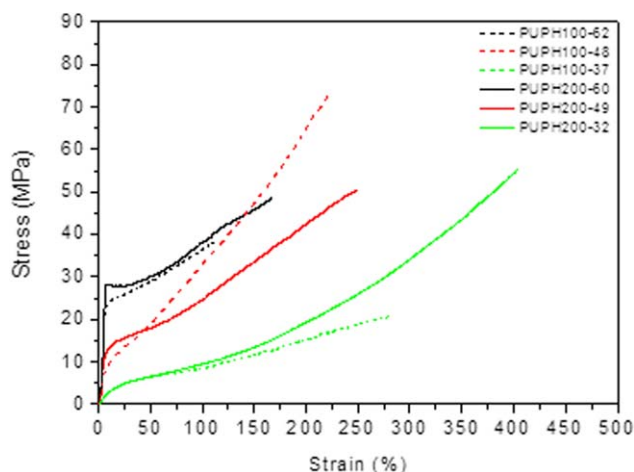
Figure 8. Stress–strain curves for the different PUs. [Color figure can be viewed in the online issue, which is available at wileyonlinelibrary.com.]

spherulite type, is similar to the one obtained by other authors.[10,30–32] These spherulites vary with the molecular weight of the soft segment and hard segment content. The spherulite size increases as the percentage of hard segment content increases. The globular domains arrangement of the sample PUPH100-37 is observed with some uncertainty and multi petal flower features are detected similar to Xu et al.[31] As the content of hard segment increases, the globular domains expand, covering almost the entire surface and increasing the connectivity between them, the dark areas related to the soft phase nearly disappears. Interactions between hard segments are so strong that during the casting process, hard segment chains prevent migration of soft segment surface. For the samples with low hard segment content small domains with less interconnectivity are observed delimited by a soft matrix increasingly visible. In this situation, the interaction forces between the hard segments are less strong and the soft segment has a higher mobility, can penetrate through the hard segments and migrate to the surface.

The mechanical properties of PUs are strongly related with the amount, size, and shape of the hard domains[20,25,33] and their intermolecular bonding, the miscibility between hard and soft segment and the possibility of the soft domains to crystallize under strain. Stress–strain curves for the different PUs are shown in Figure 8. The shape of the curves show a wide range of mechanical properties ranging from the typical behavior of

elastomeric materials with high deformation and low tensile stress at break for PUPH100-37 with low hard-segment content, to the typical behavior of thermoplastics with low deformation and high values of tensile stress for PUPH100-62 with high hard-segment content. Tensile stress increases and percentage of elongation decreases with the increase in hard-segment content. The elongation at break decreases as the hard segment increases.

Values of tensile stress at different deformations, tensile stress and strain values at break are summarized in Table IV. The polymer becomes more rigid as the hard-segment content increases making it difficult to stretch, accounting for reduced elongation. The hard-segment content is critical for the tensile behavior. Higher the hydrogen bonding is among the material and the better the phase segregation is, the harder the material is. Tensile stress increases as the hard-segment content increases. The deformation at break decreases as the hard-segment content indicating a lost in the ability of the elastomeric material. The higher initial slope of the curve and the higher tensile strength for the sample observed PUPH100-48 may be associated with greater miscibility found for this sample. As established in the literature, greater phase miscibility provides hydrogen bonding between hard and soft segment and can be reflected in an increase in tensile strength.[34,35] In PUPH200-X system, there is a slight decrease in tensile strength in contrast to the system PUPH100-X. The elongation at break decreases with hard-segment content indicating a significant decrease in the elastomeric behavior analogously to PUPH100-X. This decrease in the strain at break and the tensile strength might be related to the increase in phase segregation observed for this system with the increase in hard-segment content. By comparing the two systems, a higher elastomeric behavior with higher values of deformation at break is found in the system PUPH200-X.

Table V compiles values of tear strength, hardness, and specific gravity that increase in both systems with increase in the hard-segment content. The increase in hardness with increasing hard-segment content is due to the formation of more developed microdomains of hard segment, as observed by FTIR, DSC, and DMA, providing crossover points on the material, reinforcing the soft matrix and increasing the hardness of the polyurethane. The initial slope of the tensile properties curves agree with the values of hardness obtained. Values of relative density increase with the hard-segment content in the two systems which may be related to a better arrangement of the hard-segment and soft-segment microdomains.

Table IV. Tensile Properties

	Tensile Stress at				Tensile Properties at break	
Polyurethane	100%	200%	300%	400%	Tensile stress (MPa)	Strain (%)
PUPH100-37	8.4 ± 0.1	14.9 ± 0.3	–	–	19 ± 2	260 ± 36
PUPH100-48	34 ± 1.0	65.7 ± 0.8	–	–	75 ± 10	222 ± 24
PUPH100-62	37.5 ± 0.9	–	–	–	39 ± 1	111 ± 7
PUPH200-32	9.2 ± 0.3	19 ± 1	33.2 ± 0.9	49 ± 7	50 ± 5	401 ± 25
PUPH200-49	24.5 ± 0.5	41.7 ± 0.6	–	–	46 ± 2	232 ± 15
PUPH200-60	38.4 ± 0.3	–	–	–	45 ± 3	145 ± 22

Table V. Tear Strength Properties, Hardness, and Specific Gravity of the Polyurethanes Studied

Polyurethane	Tear strength (MPa)	Hardness Shore A Shore D		Specific gravity (g/cm^3)
PUPH100-37	66 ± 1	87	–	1.16 ± 0.03
PUPH100-48	154 ± 1	91	–	1.222 ± 0.004
PUPH100-62	133 ± 2	–	67	1.25 ± 0.04
PUPH200-32	85 ± 2	86	–	1.198 ± 0.006
PUPH200-49	118 ± 2	93	–	1.231 ± 0.005
PUPH200-60	159 ± 3	–	65	1.25 ± 0.02

CONCLUSIONS

Two series of segmented thermoplastic PUs with two macrodiols of various molecular weights and three different hard-segment contents have been synthesized via a two- step polymerization process. The FTIR and DSC results showed that the increase in the macrodiol molecular mass contributes to a decrease in the phase mixing between hard and soft microdomains. As the hard-segment content increases in each system, an increase in the bonded urethane contribution with a progressively increase in the melting temperatures and enthalpies due to the formation of larger crystalline structures of hard segment has been detected. As observed by using atomic force microscopy (AFM), both systems show a phase segregation structure of hard-/soft-segment microdomains surface which is dependent on the macrodiol molar mass and hard-segment content. X-ray diffraction did not detected crystalline structures what could be associated with the signal technique limitation.

The thermodynamic behavior is very sensitive to the macrodiol molar mass and to the hard-segment content. An increase in the hard-segment content implies an increase in the storage modulus, a decrease in the maximum peak intensity of the loss modulus as well as a decrease in the dissipation factor due to physical cross-linking points provided by the hard-segment microdomains. This trend agrees the higher mechanical properties with higher hard segment.

ACKNOWLEDGMENTS

REFERENCES

1. Szycher, M. In Handbook of Polyurethanes; CRC Press: Washington, DC, **1999**.

2. Prisacariu, C. In Polyurethane Elastomers: From Morphology to Mechanical Aspects; Springer: New York, **2011**.

3. Król, P. *Prog. Mater. Sci.* **2007**, *52*, 915.

4. Strawhecker, K. E.; Hsieh, A. J.; Chantawansri, T. L.; Kalcioglu, Z. I.; Van Vliet, K. J. *Polymer* **2013**, *54*, 901.

5. Costa, V.; Nohales, A.; Félix, P.; Guillem, C.; Gómez, C. M. *J. Elastom. Plast.* **2012**, *45*, 217.

6. Badgi, K.; Molnár, K.; Sajó, I.; Pukánszky, B. *Express Polym. Lett.* **2011**, *5*, 417.

7. Fernández d'Arlas, B.; Rueda, L.; De la Caba, K.; Mondragon, I.; Eceiza, A. *Polym. Eng. Sci.* **2008**, *48*, 519.

8. Chang, A. L.; Briber, R. M.; Thomas, E. L.; Zdrahala, R. J.; Critchfield, F. E. *Polymer* **1982**, *23*, 1060.

9. Kim, H. D.; Huh, J. H.; Kim, E. Y.; Park, Ch. Ch. *J. Appl. Polym. Sci.* **1998**, *69*, 1349.

10. Eceiza, A.; Martín, M. D.; de la Caba, K.; Kortaberria, G.; Gabilondo, N.; Corcuera, M. A.; Mondragon, I. *Polym. Eng. Sci.* **2008**, *48*, 297.

11. Lee, D. K.; Tsai, H. B.; Tsai, R. S.; Chen, P. H. *Polym. Eng. Sci.* **2007**, *47*, 695.

12. Kultys, A.; Rogulska, M.; Pikus, S.; Skrzypiec, K. *Eur. Polym. J.* **2009**, *45*, 2629.

13. Leung, L. M.; Koberstein, J. T. *Macromolecules* **1986**, *19*, 706.

14. Hu, W.; Koberstein, J. T. *J. Polym. Sci. Polym. Phys.* **1994**, *32*, 437.

15. Kojio, K.; Nonaka, Y.; Masubuchi, T.; Furukawa, M. *J. Polym. Sci. Polym. Phys.* **2004**, *42*, 4448.

16. Tanaka, H.; Kunimura, M. *Polym. Eng. Sci.* **2002**, *42*, 1333.

17. Wang, C. B.; Cooper, S. L. *Macromolecules* **1983**, *16*, 775.

18. Coleman, M. M.; Lee, K. H.; Skrovanek, D. J.; Painter, P. C. *Macromolecules* **1986**, *19*, 2149.

19. Tsai, Y. M.; Yu, T. L.; Tseng, Y. H. *Polym. Int.* **1998**, *47*, 445.

20. Spirkova, M.; Pavlicevic, J.; Strachota, A.; Poreba, R.; Bera, O.; Kapralkova, L.; Baldrian, J.; Slouf, M.; Lazic, N.; Budinski-Simendic, J. *Eur. Polym. J.* **2011**, *47*, 959.

21. Chen, T. K.; Chui, J. Y.; Shieh, T. Sh. *Macromolecules* **1997**, *30*, 5068.

22. Harris, R. F.; Joseph, M. D.; Davidson, C.; Deporter, C. D.; Dais, V. A. *J. Appl. Polym. Sci.* **1990**, *41*, 487.

23. Harris, R. F.; Joseph, M. D.; Davidson, C.; Deporter, C. D.; Dais, V. A. *J. Appl. Polym. Sci.* **1990**, *41*, 509.

24. Kim, H. D.; Lee, T. J.; Huh, J. H.; Lee, D. J. *J. Appl. Polym. Sci.* **1999**, *73*, 345.

25. Wang, T. L.; Huang, F. J. *Polymer* **2000**, *41*, 5219.

26. Bengtson, B.; Feger, C.; Macknight, W. J. *Polymer* **1985**, *26*, 895.

27. Bonart, R.; Morbitzer, L.; Hentze, G. *J. Macromol. Sci. B.* **1969**, *B3*, 337.

28. Trovati, G.; Sanches, E. A.; Neto, S. C.; Mascarenhas, Y. P.; Chierice, G. O. *J. Appl. Polym. Sci.* **2010**, *115*, 263.

29. Merline, J. D.; Nair, C. P. R.; Gouri, C.; Bandyopadhyay, G. G.; Ninan, K. N. *J. Appl. Polym. Sci.* **2008**, *107*, 4082.

30. Fridman, I. D.; Thomas, E. L. *Polymer* **1980**, *21*, 388.

31. Xu, M. X.; Liu, W. G.; Wang, C. L.; Gao, Z. X.; Yao, K. D. *J. Appl. Polym. Sci.* **1996**, *61*, 2225.

32. Mishra, A.; Maiti, P. *J. Appl. Polym. Sci.* **2011**, *120*, 3546.

33. Ono, K.; Shimada, H.; Nishimura, T.; Yamashita, S.; Okamoto, H.; Minoura, Y. *J. Appl. Polym. Sci.* **1977**, *21*, 3223.

34. Martin, D. J.; Meijs, G.; Renwick, G. M.; Gunatillake, P. A.; McCarthy, S. J. *J. Appl. Polym. Sci.* **1996**, *60*, 557.

35. Kultys, A.; Rogulska, M.; Pikus, S. *J. Appl. Polym. Sci.* **2012**, *123*, 331.